Hypo and Hyperthyroid disorder detection from thermal images using Bayesian Classifier

Mrs. Pallavi Mahajan
Department of Instrumentation & Control,
College of Engineering for Women
Pune-411052, India
Email: pallavispatil87@gmail.com

Prof. Mrs. Swati Madhe
Department of Instrumentation & Control,
College of Engineering for Women
Pune-411052, India
Email: swatimadhe@rediffmail.com

***Abstract*—Nowadays thyroid gland disorder is very common disease. More than one third of all women may be found to have at least one thyroid nodule disorder during their lifetime. Thyroid detection test is usually done by invasive and non-invasive methods. Invasive methods like Thyroid Function Tests(TFTs), biopsy are traumatic methods and non-invasive methods like ultrasound and x-rays should not be used many time. TFT is a collective term for blood tests used to check the function of the thyroid. This is invasive method to detect thyroid gland disease. TFTs may be requested if a patient is thought to suffer from hyperthyroidism or hypothyroidism. This paper gives the state of the art of image processing techniques to detect the thyroid gland disease non- traumatically using Thermograph. Thermographs are the images taken by Thermal Imaging. Thermal Imaging is a technology that creates and analyses image by detecting the heat radiating from an object.We have proposed a system to detect the thyroid gland disease using thermograph. A hyperactive thyroid gland is a center of increased blood flow and chemical activity, so it is a center of heat production that can be detected by thermal sensing. Temperature can be sensed using thermal camera FLIR-E30 with thermal sensitivity of 0.1^0C with temperature range -20^0C to +120^0C. The images of the patients neck is captured by using thermal camera FLIR-E30. These images are filtered by using median filter, and enhanced by histogram equalization. The segmentation of the images is done done using Otsus Thresholding technique to extract the thyroid region from the image. Features are then extracted and thyroid images are classified in hypo and hyperthyroid using Bayesian Classifier.**
***Keywords*- Thermography, Thermal imaging, thyroid gland.**

I. INTRODUCTION

The thyroid is a small, butterfly-shaped gland located in the front of the neck below the larynx, or voice box as shown in Fig. 1. The thyroid gland makes two thyroid hormones, triiodothyronine (T3) and thyroxine (T4), which circulates in the blood-stream and act on virtually every tissue and cell in the body. Thyroid hormone production in the thyroid is regulated by another hormone called thyroid-stimulating hormone (TSH). TSH is made by the pituitary gland, which is located in the brain.

A thyroid gland is a center of increased blood flow and chemical activity, so it a center of heat production that can be detected by thermal sensing [1]. There are two types of thyroid disorders, Hypothyroid and Hyperthyroid. The mean skin temperature where the thyroid is located of normal person is 35.76$\pm$0.49^0C. The mean skin temperature where the thyroid is located of hyperthyroidism is 36.63$\pm$0.56^0C and Hypothyroidism is 34.93$\pm$0.32^0C [2]. Basically the emissivity of human skin is high therefore the measurement of IR radiation emitted by skin can be directly converted to temperature. Temperature can be sensed using thermal camera FLIR-E30. The colored images of neck of 44 thyroid patients and normal persons are compared to classify the thyroid disorder in hyperactive, hypoactive or normal range. The images are capture by using thermal camera FLIR-E30. These images are filtered using median filter and enhanced by using histogram equalization. For detection of area, segmentation is done by using thresholding technique. ROI is manually extracted from the probable thyroid region and then resized with a size of M x M matrix. Various feature extraction methods are used and analysed. Out of these five discriminative textural features extracted from the selected ROIs: Haar Wavelet, Local Coefficient Variation(LCV), Block Difference of Inverse Probability(BDIP), Normalised Multiscale Intensity Difference(NMSID) and area, these features are applied to Bayesian Classifier is to classify the database in to hypo and hyperthyroid patients. The rest of this paper is organized as follows. Section II gives block diagram of system and details of steps and Section III gives the experiment results. Conclusions are given in Section IV.

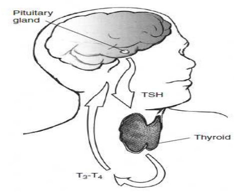

Fig. 1. Thyroid Gland Anatomy

II. BLOCK DIAGRAM OF SYSTEM

Fig. 2 shows the block diagram of the system. First we take the coloured images of neck of thyroid patients by using thermal camera FLIR E-30. These images are filtered using median filter and enhanced by using histogram equalization. For detection of area, segmentation is done by using thresholding technique. Features are then extracted and these features

978-1-4799-7319-4/14/$31.00 2014 IEEE

are applied to Bayesian Classifier to classify the hypo and hyperthyroid.

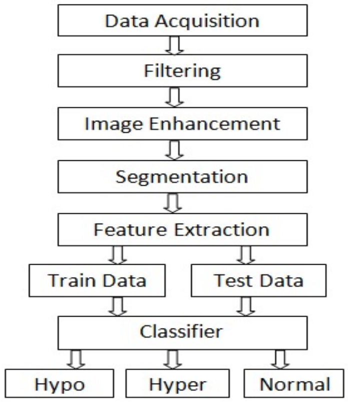

Fig. 2. Block Diagram

A. Data Acquisition

Infra-red energy coming from an object is focused by the optics onto an infra-red detector. The detector sends the information to sensor electronic for image processing. The electronics translate the data coming from the detector into an image that can be viewed in the viewfinder or on a standard video monitor or LCD screen [6]. The FLIR E-30 is easy to use and offers a temperature range of -20 to 250^0C (-4 to 482^0F) with an accuracy of $\pm 2\%$ and a thermal sensitivity of ¡0.10^0C. The 160 x 120 pixel resolution provides impressive infra-red image quality. The manual focus lens provides a 25^{0}x19^0 field of view [6]. In Fig. 3(a) shows thermal image of normal person and (b) shows thermal image of person having thyroid disorder obtained from IR camera FLIR E-30. Thyroid

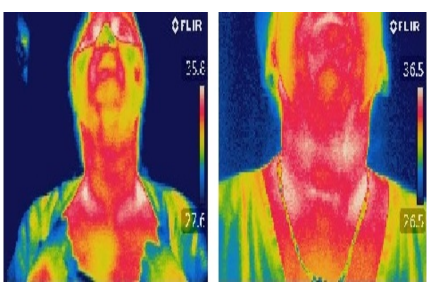

Fig. 3. (a) Normal & (b) Abnormal Persons

Thermography is a 15 min non-invasive test of physiology. It is a valuable procedure for alerting the doctor to the changes that can indicate early stage thyroid disorder. The neck area is cooled with an air conditioner for approximately 10-15 min during the image capturing process. The room temperature is adjusted approximately 22^0C and darkened during the test to minimize infra-red source interferences.

B. Image Filtering

Median filtering is a non-linear method used to remove noise from images [5]. Noise is present in the thermal image for removing this noise median filter is used. It is widely used as it is very effective at removing noise while preserving edges. It is particularly effective at removing salt and pepper type noise. The median filter works by moving through the image pixel by pixel, replacing each value with the median value of neighbouring pixels. The pattern of neighbours is called the window, which slides, pixel by pixel over the entire image. The median is calculated by first sorting all the pixel values from the window into numerical order, and then replacing the pixel being considered with the middle (median) pixel value. The input pixel is replaced by the median of the pixels contained in a window around the pixel [5]. Fig. 4 (a) shows Gray image and (b) shows result of median filter.

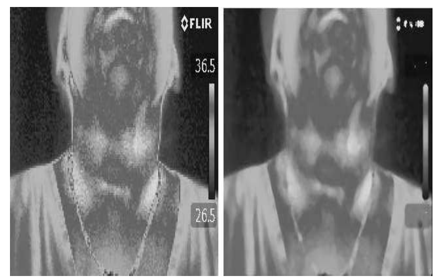

Fig. 4. (a) Original image & (b) Output of Median filter

C. Image Enhancement

Image enhancement refers to accentuation, or sharpening, of image feature such as edge boundaries or contrast to make a graphic display more useful for display and analysis [5]. The Enhancement techniques like contrast limited adaptive histogram equalization, histogram equalization and decorrelation were implemented but The Histogram Equalization is used in this work because the result of histogram equalisation is better than other techniques. Fig. 5 (a) shows result of median filter and (b) shows result of histogram equalization.

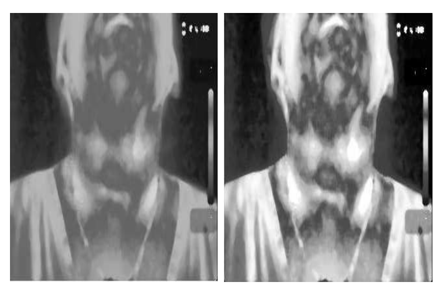

Fig. 5. (a) Output of Median filter & (b) Histogram Equalised Image

D. Image Segmentation

In this work, ROI is extracted manually from the probable thyroid region. Image is binarized by using Otsus Thresholding method. Thresholding is used to extract an object from its background by assigning an intensity value T (threshold) for each pixel is either classified as an object point or a background point. Otsus Thresholding chooses the Threshold to minimize the interclass variance of the thresholded black and white pixels. In Fig. 6 (a) shows ROI and (b) shows result of Otsus Thresholding.

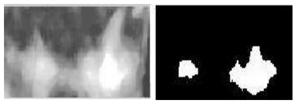

Fig. 6. (a) ROI & (b) Thresholded Image

The within interclass variance is defined as,

$$\sigma^2_{within}(T) = \omega_B(T)\sigma^2_B(T) + \omega_0(T)\sigma^2_0(T)$$

where,

$$\omega_B(T) = \sum_{i=0}^{L-1} P(i)$$

[0, L-1]the range of intensity levels.

$$\omega_0(T) = \sum_{i=0}^{L-1} P(i)$$

$\sigma^2_B(T)$ = the variance of pixels in the background(below threshold)
$\sigma^2_0(T)$ = the variance of pixels in the foreground(above threshold)
Here the optimal threshold is taken to be 0.85 for all images (Normal/ Abnormal).

E. Feature Extraction

Various feature-extraction methods have been implemented and analysed, out of these five discriminative textural features were then extracted from the selected ROIs: These features are applied to Bayesian Classifier to classify the features. These features are described in more detail as follows.

1) Haar Wavelet Features: The mean and the variance of the low-low-frequency sub-band (LL band) were computed as follows:

$$\text{Mean of LL band}(\mu) = \frac{1}{M^2} \sum_{(x,y)\epsilon B} I(x,y)$$

$$\text{Variance of LL band}(\sigma^2) = \frac{1}{M^2} \sum_{(x,y)\epsilon B} (I(x,y) - \mu)^2$$

where, *I(x, y)* denotes the intensity of a pixel*(x, y)* in the ROI block, which has passed through the Haar Wavelet, and B denotes a block size of M x M [7].

2) Coefficient of Local Variation Feature: The coefficient of variation (CV) is a normalized measure of dispersion of a probability distribution. Because the texture of thyroid gland differs from those of other regions in the US image, CV is a useful index to represent it [7]. The coefficient of local variation of a pixel located at (x, y) is defined as follows:

$$\text{LCV} = \frac{\sigma}{\mu}$$

where, μ and σ are the local mean and standard deviation of a pixel located at *(x, y)* with a block size of M M, respectively.

3) BDIP Feature: The BDIPs uses local probabilities in image blocks to measure local brightness variations of an image. BDIP is defined as the difference between the number of pixels in a block and the ratio of the sum of pixel intensities in the block to the maximum in the block [7].

$$\text{BDIP} = M^2 - \frac{\sum_{(x,y)\epsilon B} I(x,y)}{max_{(x,y)\epsilon B} I(x,y)}$$

where, *I(x, y)* denotes the intensity of a pixel *(x,y)* and B denotes a block with a size of M x M.

4) NMSID Feature: Normalized Multi-Scale Intensity Difference is defined as the differences between the pixel pairs with horizontal, vertical, diagonal, and asymmetric-diagonal directions.

$$\text{NMSID} = \sum_{k=1}^{n} \left[\begin{array}{c} \sum_{x=1}^{M} \sum_{y=1}^{M-k} \frac{|I(x,y)-I(x,y+k)|}{M(M-k)} + \\ \sum_{x=1}^{M-k} \sum_{y=1}^{M} \frac{|I(x,y)-I(x+k,y)|}{M(M-k)} + \\ \sum_{x=1}^{M-k} \sum_{y=1}^{M-k} \frac{|I(x,y)-I(x+k,y+k)|}{(M-k)^2} + \\ \sum_{x=1}^{M-k} \sum_{y=1}^{M-k} \frac{|I(x,M-y)-I(x,M-(y+k))|}{(M-k)^2} \end{array} \right] /4$$

where, *I(x, y)* denotes the intensity of a pixel *(x, y)* in a block with a size of M x M and n denotes the maximum horizontal or vertical distance [7].

5) Area: In Hypo, Hyperthyroid and normal image area is different therefore area is one of the important feature to extract the images. For feature extraction estimate the area of object in binary image. Input image can be numeric or logical. For numeric input, any non-zero pixels are considered to be on. Area is the pixel information present in binary image. There are six different patterns, each representing a different area:

- Patterns with zero ON pixels (area = 0)
- Patterns with one ON pixel (area = 1/4)
- Patterns with two adjacent ON pixels (area = 1/2)
- Patterns with two diagonal ON pixels (area = 3/4)
- Patterns with three ON pixels (area = 7/8)
- Patterns with all four ON pixels (area = 1)

Each pixel is part of four different 2-by-2 neighbourhoods. This means, for example, that a single ON pixel surrounded by OFF pixels has a total area of 1.

F. Classification

1) Naive Bayes Classification: Naive Bayes is a simple probabilistic classifier based on applying Bayes theorem (or Bayes rule) with strong independence (naive) assumptions.
Bayes rule:

$$P(H|E) = \frac{(P(E|H)P(H))}{(P(E))}$$

The basic idea of Bayes rule is that the outcome of a hypothesis or an event (H) can be predicted based on some evidences (E) that can be observed. Bayes rule for multiple evidences:

$$P(H|E1, E2....En) = \frac{(P(E1,E2,...,En|H)P(H))}{(P(E1,E2,.En))}$$

With the independence assumption, we can rewrite the Bayes rule as follows:

$$P(H|E1, E2...En) = \frac{(P(E1|H)P(E2|H)...P(En|H)P(H))}{(P(E1, E2, ..., En))}$$

where,
P(H)= Probability of event,
P(E)= Probability of evidence.

2) Performance of classifier: The data is extracted with features and then classify by using Bayesian Classifier. Performance of classifiers are found by using the formulas given below.

Accuracy = $\frac{(TP+TN)}{(TP+FP+FN+TN)}$
Sensitivity = $\frac{TP}{(TP+FN)}$ = Probability of + ve test given that patient is ill.
Specificity = $\frac{TN}{(TN+FP)}$ = Probability of - ve test given that patient is well.

where,
TP = True Positive
FN = False Negative
FP = False Positive
TN = True Negative
Table No.I shows Performance of Bayesian classifier.

TABLE I

Classifier	Accuracy	Sensitivity	Specificity
Bayesian	81.81%	93.33%	100%

III. Results

Table no. II shows the results of five features Haar Wavelet, LCV, BDIP, NMSID, Area and doctor's opinion and results of Bayesian classifier. There are total 44 persons, 30 abnormal persons and 14 normal persons from these 22 persons given to train data set and 22 persons given to test data set of Bayesian Classifier. Table no II shows some of the results of feature extraction out of 22 and table no.III shows doctor's opinion and result of Bayesian Classifier. In the result of Bayesian Classifier there are 5 hyperthyroid, 9 hypothyroid and 7 normal persons compare with doctor's opinion.

TABLE II

No.	Img No.	Haar Wavelet Mean	Haar Wavelet Variance	LCV	BDIP	NMSID	Area
1	DB1	326.637	8.63E+3	0.284	1.43E+5	0.0297	1451
2	DB2	285.773	7.49E+3	0.302	1.01E+5	0.0623	570.5
3	DB3	291.473	1.03E+4	0.348	1.06E+5	0.0495	824
4	DB4	377.800	3.73E+3	0.161	2.31E+4	0.1	581
5	DB5	283.517	3.58E+3	0.210	1.01E+5	0.0728	1431
6	DB6	247.329	1.96E+3	0.178	1.04E+5	0.0845	244.2
7	DB7	276.646	3.11E+3	0.201	1.05E+5	0.0493	896.5
8	DB8	280.496	3.49E+3	0.210	1.59E+5	0.0336	1537.5
9	DB9	261.523	1.62E+3	0.153	1.20E+5	0.0237	170
10	DB10	285.039	2.04E+3	0.158	7.63E+4	0.1	31.75
11	DB11	312.552	7.03E+3	0.268	9.03E+4	0.062	412.12
12	DB12	298.325	6.13E+3	0.262	9.28E+4	0.1	164.87

TABLE III

No.	Img No.	Doctor's opinion	Result of Baysian
1	DB1	Hypo	Hyper
2	DB2	Hyper	Hyper
3	DB3	Hypo	Hypo
4	DB4	Hypo	Normal
5	DB5	Hyper	Hyper
6	DB6	Hypo	Hypo
7	DB7	Hypo	Hyper
8	DB12	Hypo	Hyper
9	DB13	Hypo	Hypo
10	DB16	Normal	Normal
11	DB17	Normal	Normal
12	DB18	Normal	Normal

IV. Conclusion

Bayesian Classifier gives 81.81% accuracy to classify the Hypothyroid, Hyperthyroid and Normal persons. Therefore thermography could be the best technique to detect thyroid gland disease as it is noncontact, noninvasive, nontraumatic and simple method of mapping the body skin temperatures.

Acknowledgement

I am extremely grateful to my guide Mrs. Swati Madhe for providing me with best facilities and atmosphere for the creative work guidance and encouragement. I would like to thank Prof. Dr. Ashok Gaikwad, Head of Instrumentation and Control Department for all help and support extended to me. I would also like to thank Prof. Dr. Madhuri Khambete, Principal of Cummins College of Engineering for Women for her support.

References

[1] Adhy Helmy, Michael Holdman, and Maher Rizkalla, "Application of thermography for noninvasive diagnosis of thyroid gland disease", *IEEE Trans.Biomed. Eng.* vol.55, no3, March2008.
[2] Aweda M.A, Adeyomoye A.O, Abe G.A, "Thermographic analysis of thyroid disease", *Adv. Appl. Sci. Res*,2012,3(4) 2027-2032.
[3] F.H.Y. Chan, A.T.P. So, A.W.C. Kung,t F.K. Lam and H.C.L. Yip, "Thyroid Diagnosis by Thermogram Sequence Analysis", *Elsevier Science Ltd. Bio-Medical Materials and Engineering*, Vol. 5, No. 3, pp. 169-183, 1995
[4] Anil k. Jain, "Fundamentals of Digital Image Processing", Eastern Edition 2005.
[5] Rafeal c. Gonzalez, Richard E. Woods, Steven E. Eddins, "Digital Image Processing Using MATLAB", Second Edition 2010..
[6] FLIR E-30 Datasheet.
[7] Chuan-yu Chang. Yue-fong Lie, Chin, Shyang-rong, "Thyroid Segmentation and Volume Estimation in US Images", *IEEE Transactions on Biomedical Engineering*, Vol. 57, No.6, June 2010.